

Layer splitting process in hydrogen-implanted Si, Ge, SiC, and diamond substrates

Q.-Y. Tong,^{a),b)} K. Gutjahr, S. Hopfe, and U. Gösele^{b)}
Max-Planck-Institute of Microstructure Physics, Weinberg 2, D-06120 Halle, Germany

T.-H. Lee
Wafer Bonding Laboratory, Duke University, Durham, North Carolina 27708

(Received 13 November 1996; accepted for publication 10 January 1997)

Si, Ge, SiC, and diamond samples were implanted with H_2^+ at 120–160 keV with 5.0×10^{16} ions/cm² (corresponding to 1.0×10^{17} H^+ ions/cm²) and annealed at various temperatures to introduce hydrogen filled microcracks. An effective activation energy was determined for the formation of optically detectable surface blisters from the time required to form such blisters at various temperatures. The measured effective activation energies are close to the respective bond energies in all four materials. The time required to completely split hydrogen implanted layers from bonded silicon substrates and to transfer them onto oxidized silicon wafers is a factor of about 10 longer. Both processes, blister formation and layer splitting, show the same activation energy.
© 1997 American Institute of Physics. [S0003-6951(97)03211-7]

Layer transfer from a hydrogen-implanted wafer onto a desirable substrate by wafer bonding and layer splitting is an attractive approach to form SOI (silicon-on-insulator)¹ or other material combinations such as SiC on oxidized silicon.² The substrate from which the hydrogen implanted layer is split can be reused, and a good thickness uniformity of the split layer is achieved by the hydrogen implantation. An understanding of the layer-splitting behavior of hydrogen-implanted materials which is just emerging for the case of silicon,³ is vital to implement the layer transfer approach for different material combinations. We investigated the behavior of hydrogen implanted materials consisting of group IV elements (Si, Ge, diamond) or one of their compounds (SiC). All of these materials including diamond⁴ can be bonded to mirror-polished substrates, provided these materials are mirror polished themselves or covered with appropriate intermediate layers (such as a SiO₂ layer) which has been polished. Layer splitting and transfer to a substrate requires the combination of wafer bonding and the development of hydrogen-induced microcracks extending parallel to the bonding interface during a subsequent annealing step. In this letter, we report the effective activation energies of the times required to form hydrogen-induced surface blister in unbonded samples or to accomplish layer splitting in bonded samples, and the different time requirements for these two processes. Based on these observations a speculative layer splitting mechanism is suggested. The application of the approach to realize a SiC layer on a high-temperature glass is also briefly mentioned.

The material and implantation parameters of the single crystalline Si, Ge, SiC, and diamond used in this study are listed in Table I. The maximum temperature during the implantation was controlled to stay below 200 °C.

To investigate hydrogen-induced microcrack formation, the hydrogen implanted Si, Ge, and SiC wafers were cut into small pieces of about 2×7 mm which were then annealed at various temperatures in air. The diamond samples of 3 mm

in diameter with 1.2 mm in thickness were annealed in nitrogen to prevent graphitization which starts at ~500 °C in an oxidizing ambient. In order to achieve a high accuracy, the furnace temperature was preset before the samples were put in and the samples were taken out of the furnace rapidly at the end of the annealing time and quickly cooled down to room temperature as their thermal capacities are very small. Optical microscopy and cross-sectional transmission electron microscopy (TEM) were used for detection of hydrogen microcrack formation. An example of a microcrack in Ge is shown in the cross-sectional TEM picture of Fig. 1. In most cases of unbonded implanted materials, bulges or blisters appeared on the surface of the samples after appropriate annealing. Such features with a diameter of about 2.5 μm can easily be detected by an optical microscope with a magnification of 400. For convenience, we defined this stage as the onset of optically detectable microcrack formation.

Hydrogen implanted Si wafers were also directly bonded at room temperature to Si wafers covered with 1 μm thermal oxide and annealed at 160 °C to enhance the bond energy before the bonded wafers were treated at various temperatures to split the implanted layers. SOI structures were also realized for entire 4 in. wafers. Small pieces as well as whole 1.375 in. hydrogen implanted SiC wafers were anodically bonded to a high-temperature glass which was specifically developed at the Max-Planck Institute of Solid State Research in Stuttgart with a thermal expansion coefficient close to silicon and is stable up to about 800 °C.⁵ The bonded SiC/glass pairs were thermally treated at 725 °C to split the hydrogen implanted SiC layers onto the glass substrates. These experiments will be published in detail elsewhere.⁶ Hydrogen implanted Ge layers were also transferred to glass substrates by anodic bonding and layer splitting.

The times required to form hydrogen-induced microcracks which were sufficiently large to lead to optically detectable surface blisters on the Si, Ge, SiC, and diamond samples was determined at various temperatures as shown in Fig. 2. From Fig. 2 the effective activation energies E_a for the time t_b to form optically detectable hydrogen surface blisters in the various materials are derived based on

^{a)}Electronic mail: material@acpub.duke.edu

^{b)}Also at: Wafer Bonding Laboratory, Duke University, Durham, NC 27708.

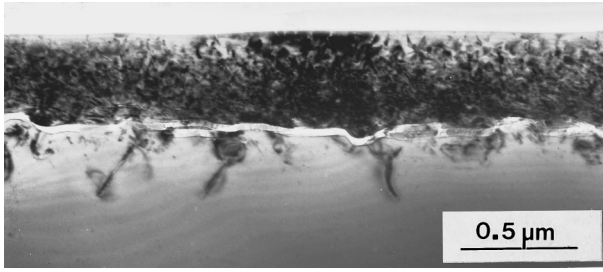


FIG. 1. Cross-sectional TEM image of microcrack in Ge after H_2^+ implantation at 160 keV with 5.0×10^{16} ions/cm² and annealing at 300 °C for 1 h.

$$1/t_b \propto \exp(-E_a/kT),$$

where k is Boltzmann's constant, T the absolute temperature, and is compared with the bond energies of Si-Si, Ge-Ge, Si-C, and C-C (diamond) in Table II.

After hydrogen implantation, the originally hydrophilic surfaces of the silicon wafers had changed into being strongly hydrophobic. In contrast to normal hydrophobic Si wafer surfaces which are formed by a dip in dilute HF, the surfaces of the H-implanted silicon wafers remain hydrophobic after RCA1 cleaning for 10 min at 85 °C. Immersion of the RCA cleaned wafers in water for more than 15 h at room temperature is required to convert the surfaces back to a hydrophilic state. It is believed that implanted hydrogen can break Si-Si bonds and react with silicon to form a hydrogen terminated surface with passivated surface vacancies.⁷ The unusually high surface concentration of hydrogen may be attributed to the additional trapping at implantation-induced surface defects.⁸ Similar effects were also observed in the case of Ge wafers. The time required to convert the surfaces from hydrophobic to hydrophilic by immersing in water was even longer for Ge wafers.

It is known⁹ that even at room-temperature implanted hydrogen in bulk Si can react with broken Si-Si bonds at implantation-induced defects to form Si-H bonds. Moreover, the implanted hydrogen leads to the formation of planar defects or platelets which later on develop into microcracks. In order to check whether there is a difference in hydrogen blister formation between implantations with H^+ and with H_2^+ , in a separate set of experiments the two ions with approximately equivalent implant conditions (H^+ : 60 keV, 1.0×10^{17} ions/cm²; H_2^+ : 120 keV, 5.0×10^{16} ions/cm²) were implanted into silicon. No differences in blister formation were found at temperatures above 218 °C.

It is believed that the H_2^+ ion splits upon impact with the Si wafer surface, coming to rest as a hydrogen atom.

For the H-implanted Si/oxidized Si bonded pairs, the time required to completely split the H-implanted layers from the silicon substrates and transfer them onto the oxidized silicon wafers at various temperatures was measured. The results are shown in Fig. 3. Compared with the time needed to form hydrogen microcracks leading to optically detectable surface blisters, the time for large area layer splitting after bonding is about ten times longer. However, the effective activation energies for the two procedures are basically the same as can be seen from Fig. 3 which indicates that the same atomistic process also dominates the layer-splitting stage. The method and results shown in Figs. 2 and 3 can serve as design guidelines of process windows for the layer transfer approach.

There appears to exist a minimum critical temperature for each H-implanted material below which the time to form hydrogen-induced surface blisters is much longer than that predicted by the respective effective activation energies. As can be seen in Fig. 1, for silicon the critical temperature is about 218 °C, for Ge ~200 °C, for SiC ~650 °C, and for diamond ~850 °C. The explanation for this phenomenon is still under investigation.

So far, the materials for which we were able to detect microcrack generation in sufficient amount to allow formation of optically detectable surface blisters after hydrogen implantation and annealing are group IV elements or compounds. Other materials investigated such as GaAs, InP, or Al₂O₃ have failed to show the same blistering phenomenon in unbonded samples. For these materials the use of helium implantation¹⁰ with higher doses might lead to successful layer splitting.

Let us finally speculate on the meaning of the effective activation energies E_a determined from the times to observe optically detectable surface blisters. Microscopically, initially many tiny platelets are formed which develop into microcracks. The larger and energetically more favorable microcracks grow at the expense of smaller microcracks¹¹ in terms of a kind of two-dimensional Ostwald ripening process¹² until hydrogen-filled microcracks have reached a size which can be optically detected as surface blisters. The activation energy of a usual Ostwald ripening process is associated with the sum of the activation energies of migration and formation of the diffusing species. In the case of micro-

TABLE I. Material and implantation parameters.

Parameter	Si	Ge	SiC	Diamond
Size (diam)	4-in.	3-in.	1.375 in.	3 mm
Type	<i>p</i>	<i>n</i>	<i>n</i>	<i>n</i>
Orientation	(100)	(100)	6H on-axis, Si face	(100)
Resistivity or concentration	B doped 8–12 Ω cm	undoped 5–10 Ω cm	N doped $8.6 \times 10^{17}/\text{cm}^3$	N doped $4–40 \times 10^{17}/\text{cm}^3$
Implant energy and dose	H_2^+ : 160 keV, 5.0×10^{16} ions/cm ²	H_2^+ : 160 keV, 5.0×10^{16} ions/cm ²	H_2^+ : 160 keV, 5.0×10^{16} ions/cm ²	H_2^+ : 120 keV, 5.0×10^{16} ions/cm ²

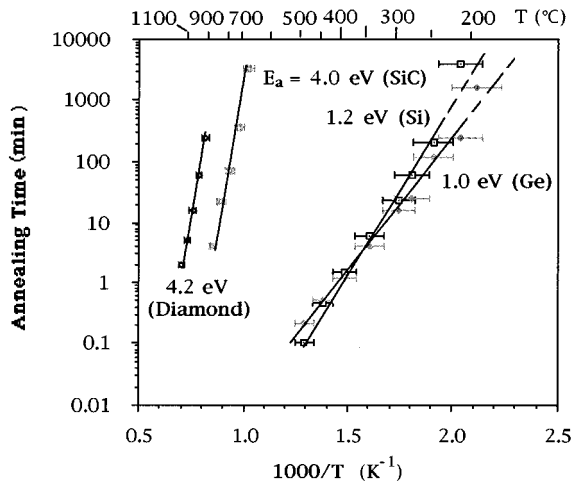


FIG. 2. Time required to form optically detectable surface blisters in hydrogen-implanted Si, Ge, SiC, and diamond as a function of annealing temperature.

cracks filled with hydrogen, no detailed theory of Ostwald ripening is available. Therefore, no comparison between theory and the observed effective activation energies has been made. In view of this complex situation it is remarkable that the observed effective activation energies E_a are close to the bond energies of the respective materials as can be seen in Table II. Whether this is a coincidence or rather indicates that bond breaking is rate limiting in the Ostwald ripening process of microcracks is presently an open question.

TABLE II. Comparison of bond energies of Si-Si, Ge-Ge, Si-C, and C-C with activation energies of microcrack formation for the Si, Ge, SiC, and diamond samples.

Material	Bond energy (eV)	Activation energy (eV)
Si	1.81	1.2
Ge	1.61	1.0
SiC	4.47	4.0
Diamond	6.19	4.2

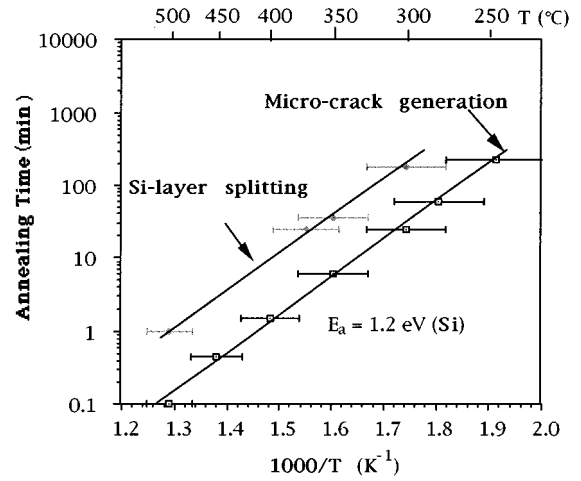


FIG. 3. Comparison between effective activation energies for the formation of optically detectable surface blisters in unbonded and for complete layer splitting in bonded hydrogen-implanted Si wafers.

The authors are grateful for support from the SEH Company.

- ¹M. Bruel, *Electron. Lett.* **31**, 1201 (1995).
- ²L. Di Cioccio, Y. Le Tiec, F. Letertre, C. Jaussaud, and M. Bruel, *Electron. Lett.* **32**, 1144 (1996).
- ³M. K. Weldon, V. Marsico, Y. J. Chabal, S. B. Christman, E. E. Chaban, D. C. Jacobson, J. B. Sapjeta, A. Pinczuk, B. S. Dennis, A. P. Mills, C. A. Goodwin, and C.-M. Hsieh, *Proc. 1996 IEEE Int. SOI Conf.* **96CH35937**, 150 (1996).
- ⁴J. Haisma, B. C. M. Spierings, U. K. P. Biermann, and A. A. van Gorkum, *Appl. Opt.* **33**, 1154 (1994).
- ⁵R. B. Bergmann, J. G. Darrant, A. R. Hyde, and J. H. Werner, *International Conference on Coating on Glass*, Oct. 27 (1996).
- ⁶Q.-Y. Tong, T.-H. Lee, U. Gösele, P. Werner, R. Brendel, R. Bergmann, and J. Werner (unpublished).
- ⁷F. Lu, J. W. Corbett, and L. C. Snyder, *Phys. Lett. A* **77**, 250 (1990).
- ⁸J. L. Lindström, G. S. Oehrlein, G. J. Scilla, A. S. Yapsir, and J. W. Corbett, *J. Appl. Phys.* **65**, 3297 (1989).
- ⁹S. J. Pearton, J. W. Corbett, and M. Stavola, *Hydrogen in Crystalline Semiconductor* (Springer-Verlag, New York, 1992), pp. 319-330.
- ¹⁰X. Lu, S. S. K. Iyer, J. Min, Z. Fan, J. B. Liu, P. K. Chu, C. Hu, and N. W. Chueng, *Proc. 1996 IEEE Int. SOI Conf.* **96CH35937**, 48 (1996).
- ¹¹A. J. Auberton-Herve, T. Barge, F. Metral, M. Bruel, B. Aspar, C. Maleville, H. Moriceau, and T. Poumeyrol, *Proceedings of 2nd International Symposium on Advanced Science and Technology Silicon Mater.* (1996), p. 214.
- ¹²Y. Kim, H. Z. Massoud, U. M. Gösele, and R. B. Fair, *Electrochem. Soc. Proc.* **91-4**, 304 (1991).